Journal of
Marine Science and Engineering

MDPI

Article

Current Status of Theoretical and Practical Research of Seawater Single-Effect Passive Solar Distillation in Mexico

Eduardo Rubio [1,*], José Luis Fernández-Zayas [2] and Miguel A. Porta-Gándara [3]

[1] Centro de Ciencias de la Ingeniería, Universidad Autónoma de Aguascalientes, Av. Universidad 940, Col. Ciudad Universitaria, Aguascalientes, Ags. 20131, Mexico
[2] Instituto de Ingeniería UNAM, Ciudad Universitaria, Coyoacán, CDMX 04510, Mexico; jfernandezz@iingen.unam.mx
[3] Engineering Group, Centro de Investigaciones Biológicas del Noroeste, La Paz, BCS 23097, Mexico; maporta@cibnor.mx
* Correspondence: erubio@correo.uaa.mx; Tel.: +52-449-910-7400

Received: 12 January 2020; Accepted: 27 January 2020; Published: 3 February 2020



Abstract: Solar distillation is a practical alternative for freshwater production in arid zones where seawater is abundant. The attractiveness of this approach resides in the simplicity of the solar still, equipment used to produce saline-free water for drinking, intensive agriculture, domestic use and other purposes. A solar still is an apparatus exposed to solar radiation that consists essentially of a basin with a solar collector where saline water is deposited and covered with a transparent inclined glass plate. The system operates as a greenhouse where the heated seawater evaporates and condensates on the inner surface of the cover. The distillate yield is collected in an external container. A research group in Mexico has been working for years doing research on the process of freshwater production with solar stills. Various research aspects have been addressed, among which are mathematical modeling of the physical phenomenon, practical research by building solar stills with different geometries and sizes, and the proposal of a process for mass-production manufacturing of solar stills with technology innovations. This paper is an overview of some of the most relevant results obtained by these research efforts.

Keywords: solar distillation; single-effect; solar energy; mathematical modeling; experimental work; innovation

1. Introduction

Maria Telkes research on solar distillation is one of the first works that addresses the topic in a formal and referenced manner [1]. In her work, published in 1953, the author offers a simplified mathematical treatment of the solar distillation process, and reports the thermal efficiency of a single-effect insulated solar still apparatus, very similar to solar stills in use today.

The main components of a single-effect solar still are shown in Figure 1. It has a thermally insulated basin with a black absorber and covered with an inclined semitransparent condenser. Seawater is deposited in the basin. Solar energy passes through the condenser and water, and reaches the absorber that raises its temperature. Water is heated by the solar energy absorbed and evaporates. The water vapor condensates when it touches the inner surface of the condenser, and runs down to a collecting channel that drains the distilled water to an external container.

The maximum efficiency of this type of solar stills is about 34%, and productivity decreases significantly with increase in depth of basin water. It has been observed that highest distillate yield is obtained with cover condenser tilted same as latitude, and that thinner glass cover thickness increases

production. Insulation plays an important role in solar distillation since it reduces heat losses through the bottom and side walls [2]. Subsequent research validates these results in similar climate [3].

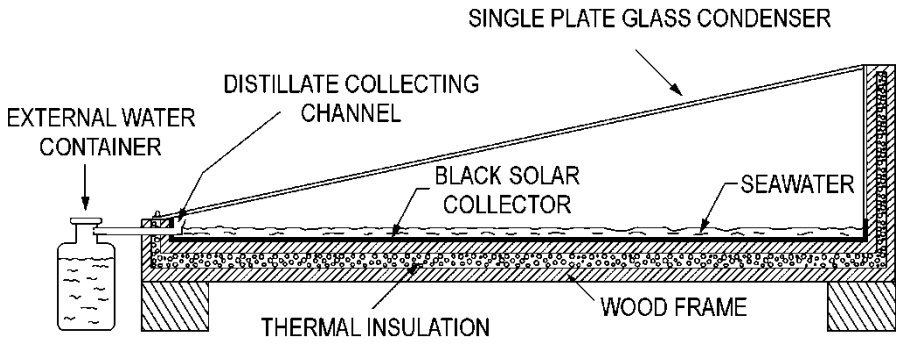

Figure 1. Single-effect single-slope condenser solar still.

2. Thermal Description of the Single-Effect Single-Slope Condenser Solar Still

Figure 2 shows the most widely used single-effect solar still where the main heat-transfer exchange modes can be observed. The characteristic feature of this still, also known as single-slope solar still, is the use of an inclined single-plate glass condenser. Mathematical relations that describe its thermal operation are based on equations that result from an energy balance obtained from a lumped-parameter analysis. For this type of apparatus, three expressions are derived concerning each of the main components of the still.

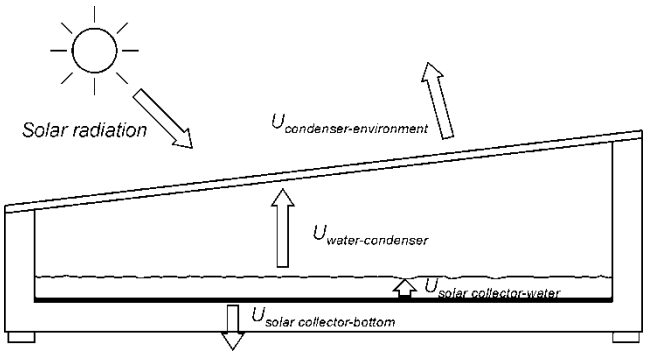

Figure 2. Heat-transfer exchange mechanisms in a solar still.

The energy balance of the still applied to the water mass, that loses energy through the bottom, and exchanges energy with the glass cover, is:

$$C_w \frac{dT_w}{dt} = H_w + U_{wb}(T_b - T_w) - U_{wg}(T_w - T_g) \quad (1)$$

The condensing plate exchanges energy with seawater and the surroundings:

$$C_g \frac{dT_g}{dt} = H_g + U_{wg}(T_w - T_g) - U_{ge}(T_g - T_e) \quad (2)$$

For the bottom absorber, the energy exchange is between the surroundings and the seawater:

$$C_b \frac{dT_b}{dt} = H_b - U_{bw}(T_b - T_w) - U_{be}(T_b - T_e) \quad (3)$$

Solar radiation incidence depends on the declination [4]:

$$\delta = 23.45 \sin\left[\frac{2\pi(284+n)}{365}\right] \tag{4}$$

Global and beam radiation can be calculated with the following expressions [5]:

$$G = G_{\max} \cos^{1.2}\left(\frac{\pi t}{N}\right) \tag{5}$$

$$G_{\mathrm{b}} = G_{\mathrm{b-max}} \cos^{1.5}\left(\frac{\pi t}{N}\right) \tag{6}$$

And the number of daylight hours is given as [6]:

$$N = \frac{2}{15}\cos^{-1}(-\tan\delta\tan\varphi) \tag{7}$$

The radiation incident on an inclined surface can be calculated as:

$$R_{\mathrm{b}} = \frac{\cos\theta}{\cos\theta_z} \tag{8}$$

For an angle between beam radiation and the normal to the plane:

$$\begin{gathered}\cos\theta = \sin\delta\sin\varphi\cos\beta - \sin\delta\cos\varphi\sin\beta\cos\gamma + \cos\delta\cos\varphi\cos\beta\cos\omega \\ + \cos\delta\sin\varphi\sin\beta\cos\gamma\cos\omega + \cos\delta\sin\beta\sin\gamma\sin\omega\end{gathered} \tag{9}$$

The beam radiation incident over a horizontal plane is:

$$\cos\theta_z = \cos\varphi\cos\delta\cos\omega + \sin\varphi\sin\delta \tag{10}$$

Optical properties are also considered from equations for transmittance, reflectance and absorptance. The transmission of energy through the glass cover is:

$$\tau_{\mathrm{a}} = \exp\left(-\frac{k_{\mathrm{ext}}L}{\cos\theta_2}\right) \tag{11}$$

Equations for estimating transmittance, absorptance and reflectance passing through semi-transparent media are:

$$\tau = \frac{\tau_a}{2}\left[\frac{1-r_\perp}{1+r_\perp}\left(\frac{1-{r_\perp}^2}{1-(r_\perp\tau_a)^2}\right) + \frac{1-r_{II}}{1+r_{II}}\left(\frac{1-{r_{II}}^2}{1-(r_{II}\tau_a)^2}\right)\right] \tag{12}$$

$$\alpha = \frac{1-\tau_a}{2}\left[\left(\frac{1-r_\perp}{1-r_\perp\tau_a}\right) + \left(\frac{1-r_{II}}{1-r_{II}\tau_a}\right)\right] \tag{13}$$

$$\rho = \frac{1}{2}[r_\perp(1+\tau_a\tau_\perp) + r_{II}(1+\tau_a\tau_{II})] \tag{14}$$

Condenser heat losses for the convective mode are [7]:

$$h_c = 2.8 + 3.0v \tag{15}$$

The radiative heat transfer exchange between the cover and the surroundings can be written as [6]:

$$h_r = \varepsilon\sigma({T_{\mathrm{g}}}^2 + {T_{\mathrm{s}}}^2)(T_{\mathrm{g}} + T_{\mathrm{s}}) \tag{16}$$

Where a sky temperature is given as [8]:

$$T_s = 0.0552 T_e^{1.5} \tag{17}$$

The basin loses heat by conduction and convection:

$$U_{be} = \left(\sum_{i=1}^{n} \frac{L_i}{k_i} + \frac{1}{h_b} \right)^{-1} \tag{18}$$

The heat exchange between the seawater mass and the blackened solar collector is calculated as [9]:

$$Nu = 0.069 Ra^{1/3} \mathrm{Pr}^{0.074} \tag{19}$$

Dunkle´s relations for convective and evaporative heat transfer in a humid environment are used when there exist simultaneously heat and mass transfer [10]:

$$h_c = 0.884 \left[T_w - T_g + \frac{P_w - P_g}{268.9 \times 10^3 - P_w} T_w \right]^{1/3} \tag{20}$$

$$h_e = 16.276 \times 10^{-3} h_c \frac{P_w - P_g}{T_w - T_g} \tag{21}$$

For the internal radiation exchange estimated as [6]:

$$h_r = \frac{\sigma \left({T_w}^2 + {T_g}^2 \right) \left(T_w + T_g \right)}{\frac{1}{\varepsilon_w} + \frac{1}{\varepsilon_g} - 1} \tag{22}$$

Recent research by the Mexican working group further discuss these findings [11].
Finally, the distillate production of the still is calculated as:

$$m'' = q_e / h_{fg} \tag{23}$$

These equations make evident the relevance of the convective mode in the heat and mass transfer that occurs in the evaporation–condensation process. This fact has been demonstrated by the authors of the present paper by experimental work. In this sense, the heat transfer coefficients for the convective and evaporative modes are shown in Figure 3. These results were made in a large cross-section solar still [12] and show the importance of the energy transport by the humid air, particularly at high temperatures. Conversely, heat transported by convection shows low values for the useful operating conditions of the still.

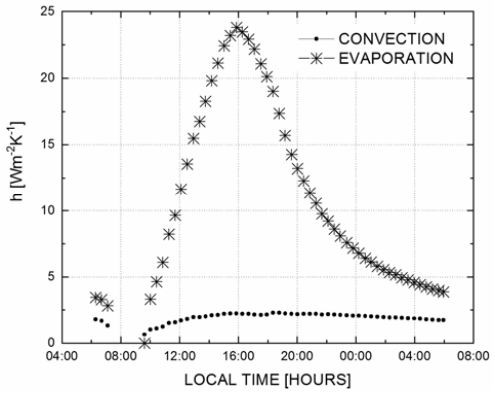

Figure 3. Relevance of the evaporative mode of heat transfer in solar distillation.

Various models to predict the mass flow rate can be found in the literature. However, there are discrepancies in predictions, as shown in Figure 4. Our model predicts higher rates of distillate, meanwhile models based on Cooper's equations estimate lower rates, and Clark's model underpredicts significantly the production due to a heat transfer coefficient defined as half of the others.

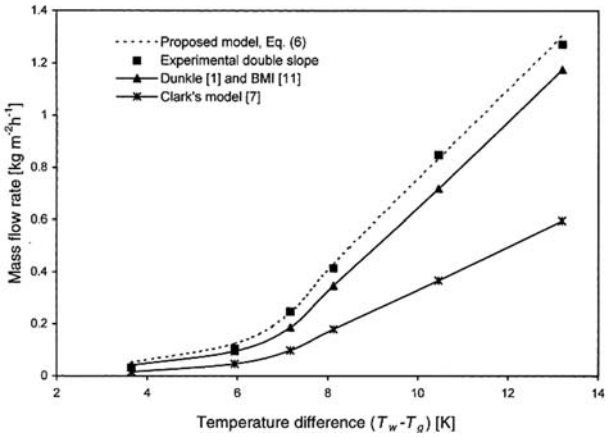

Figure 4. Distillate yield production for different mathematical models (Reprinted from [13], with permission from Elsevier, 2019).

There is a linear dependence of the production of the still on water temperature and water-to-cover temperature differences as shown in Figure 5. This plot was obtained from experimental data for a laboratory still operated under controlled conditions.

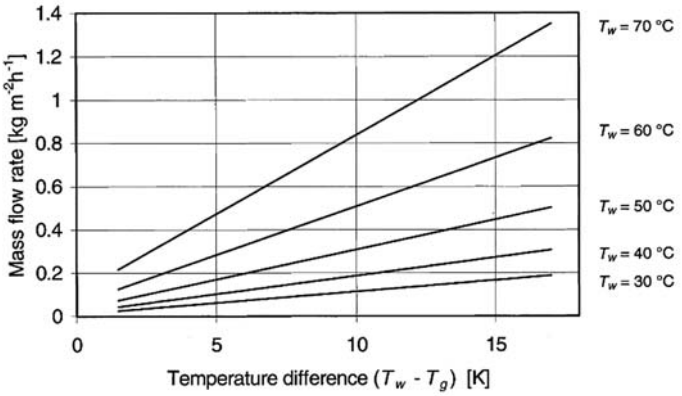

Figure 5. Temperature dependence of distillate yield on water and condensing cover temperatures (Reprinted from [13], with permission from Elsevier, 2019).

3. Single-Effect Double-Slope Condenser Solar Still

The most widely accepted model that describes the heat and mass transfer mechanisms in solar stills is found in Dunkle´s work [10]. This model was described in the previous section, and one of the considerations made is that the condenser is a single inclined plate, although the author sketches a so-called roof type solar still with an inverted-V cover condenser. Therefore, derived equations do not allow us to know the details of the performance of each plate of the condenser, since they have a different orientation.

This inverted-V geometry, that implies a condensing cover built with two inclined plates with different orientations, and therefore temperature differences, has been the subject of interest of various authors. However, a detailed analysis of its performance can not be found in the literature. The

authors of the present paper have developed modeling and experimental work on the subject, to help understand the physics of the distillation phenomena in solar stills that use this particular geometry.

Figure 6 shows a sketch of a single-effect double-slope condenser solar still. Dunkle´s model needs to be modified to be able to calculate the temperatures and distillate yield of each of the condensing plates.

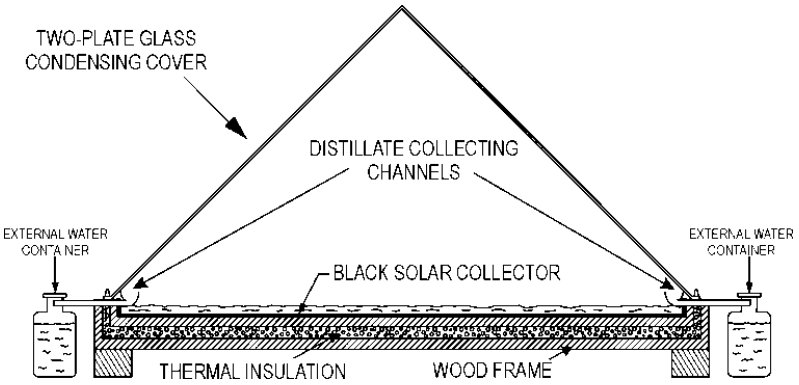

Figure 6. Sketch of a single-effect double-slope condenser solar still.

The same lumped parameter analysis applies, but energy balance equations are modified since the condensing cover is treated as composed of two independent elements for analysis purposes. This assumption gives rise to a system of four equations: Bottom absorber, water mass, and two condensing plates. Bottom absorber equation remains the same, but water exchanges energy with two condensers (g1 and g2) and with the absorber bottom:

$$C_w \frac{dT_w}{dt} = H_w + U_{wb}(T_b - T_w) - U_{wg1}(T_w - T_{g1}) - U_{wg2}(T_w - T_{g2}) \quad (24)$$

A condensing plate (g1) exchanges energy with the other condenser, seawater and environment:

$$C_{g1} \frac{dT_{g1}}{dt} = H_{g1} + U_{wg1}(T_w - T_{g1}) - U_{g1g2}(T_{g1} - T_{g2}) - U_{gle}(T_{g1} - T_e) \quad (25)$$

The equation for the second condensing plate (g2) is similar:

$$C_{g2} \frac{dT_{g2}}{dt} = H_{g2} + U_{wg2}(T_w - T_{g2}) - U_{g2g1}(T_{g2} - T_{g1}) - U_{g2e}(T_{g2} - T_e) \quad (26)$$

A Dunkle´s modified model was implemented with these equations and it is possible to know the temperatures and distillate yield of each condensing plate. The details of this new model are presented in [14]. Recent studies report the replication of this approach [15].

An engineering tool was implemented from this methodology to obtain the solar still simulator shown in Figure 7. Input parameters can be fed for basin, water, and condensing plates. Solar radiation and orientation of the still can be set, and the user can define wind and environment temperature files. The software reports plots for condensers, water and basin temperatures, and each condenser plate distillate yield.

In this solar still the humid air is confined in a triangular cavity. To gain a better understanding of its operation, numerical simulations have been carried out in this geometry. The two plates of the condensing cover have opposite orientation, and so temperature asymmetries arise that depend on the sun position. It is possible to have a differentially heated cavity, heated from below, where the temperature of one side wall is higher than the other. Under these conditions a single cell fluid flow is established as shown in Figure 8. When the cavity is heated from below, but the walls are subject to the

same temperature, a flow with two convective cells is obtained. Laboratory experiments demonstrate this fluid flow structure as shown in Figure 9.

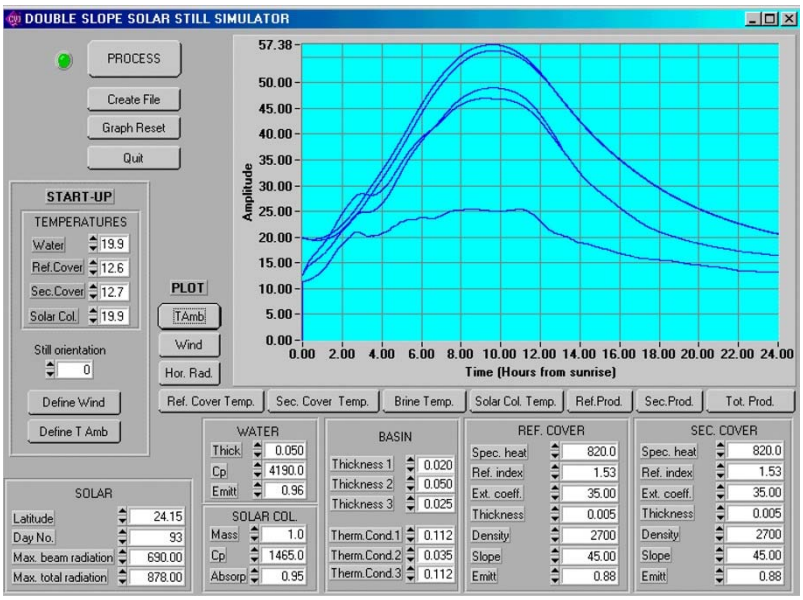

Figure 7. Computer simulator of the thermal performance of a double-slope condensing cover solar still.

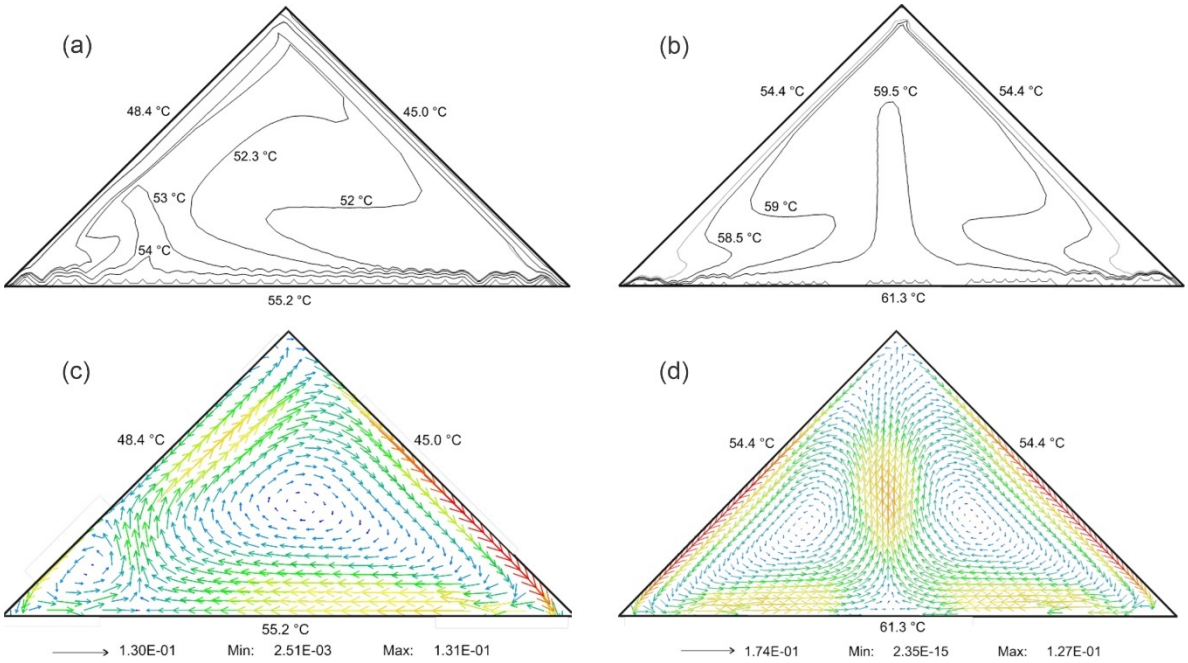

Figure 8. Isotherms (**a**) and fluid flow (**c**) in a cavity of triangular cross section heated from below with side walls at different temperatures, and isotherms (**b**) and fluid flow (**d**) for side walls at the same temperature.

In these figures a laser sheet generator was used to illuminate a section of the cavity. The two-cell flow structure, characteristic of a system heated from below with walls at the same temperatures, can be observed.

According to the temperature of the condensing plates, other authors have found that convection flows in triangular cavities are driven by a single-cell flow pattern [16]. For low turbulence flows,

this could be beneficial for the mass transfer process, as reports indicate that the peripheral layers of these flow structures have a major participation in the process of heat and mass transfer [17].

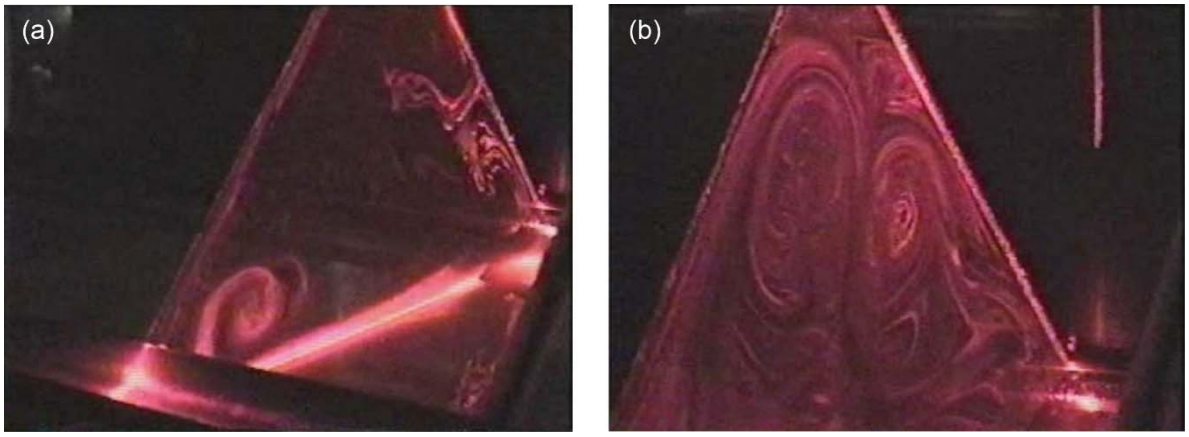

Figure 9. Visualization experiments of the convection flows in a cavity similar to those used in solar distillation. Natural convection begins (**a**) and steady-state convection (**b**).

Numerical simulations demonstrate that under certain operating conditions, the temperature of one condenser is always higher than the other, forcing the system to establish a flow characterized by a single convection cell [18].

Experimental works carried out in a double slope condenser solar still, where the temperature of each condensing plate was measured, show evident temperature differences as shown in Figure 10. The temperature trend observed in this figure is explained by the fact that when the plates are facing an east-west direction, the east facing condensing plate gets a higher temperature during sunrise, and the temperature trends are inverted after noon [19].

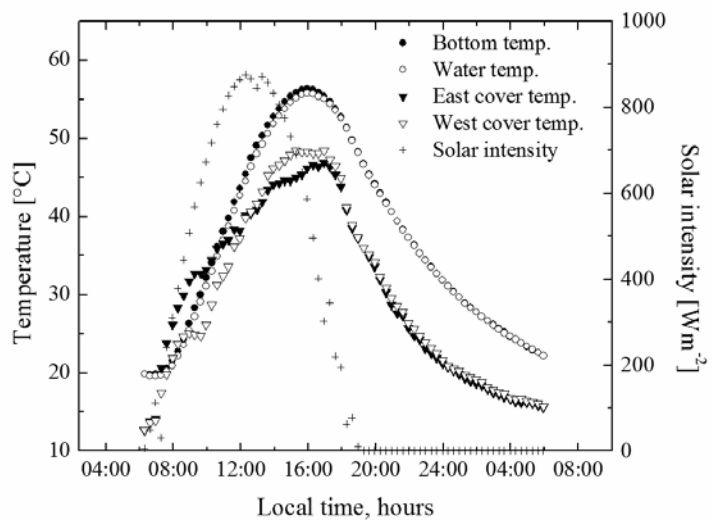

Figure 10. Experimental temperatures measured at each component of a double-slope condenser solar still (Reprinted from [19], with permission from Elsevier, 2019).

The case of the condensing plates facing an east–west direction, shows the major production differences as can be observed in Figure 11. East cover distillate yield drops to zero during sunrise because its temperature gets hotter than brine temperature due to its direct exposure to sun radiation. The distillate production asymmetries in this figure justify the development of the extended model described in this section of the paper.

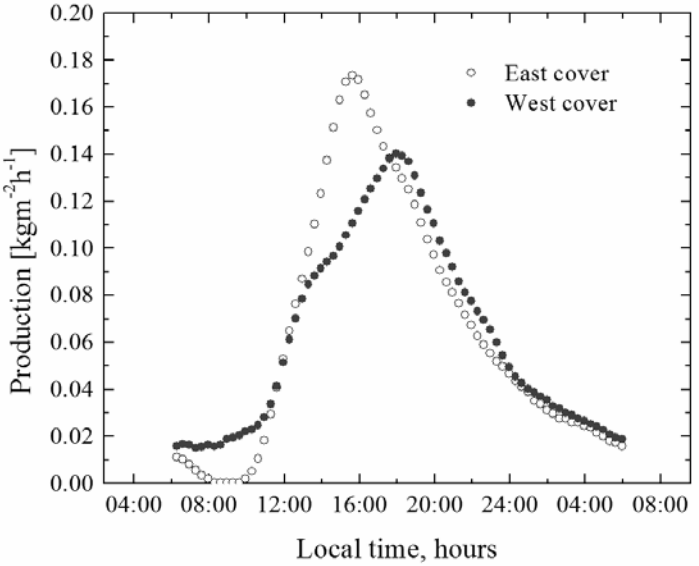

Figure 11. Distillate production with condensers facing an east–west direction in a double-slope condenser solar still (Reprinted from [19], with permission from Elsevier, 2019).

For the case when the condensing plates are facing a north-south direction there are conditions of quasi-symmetric exposure to sun rays, for which the same production trend is obtained for both condensing plates, as shown in Figure 12.

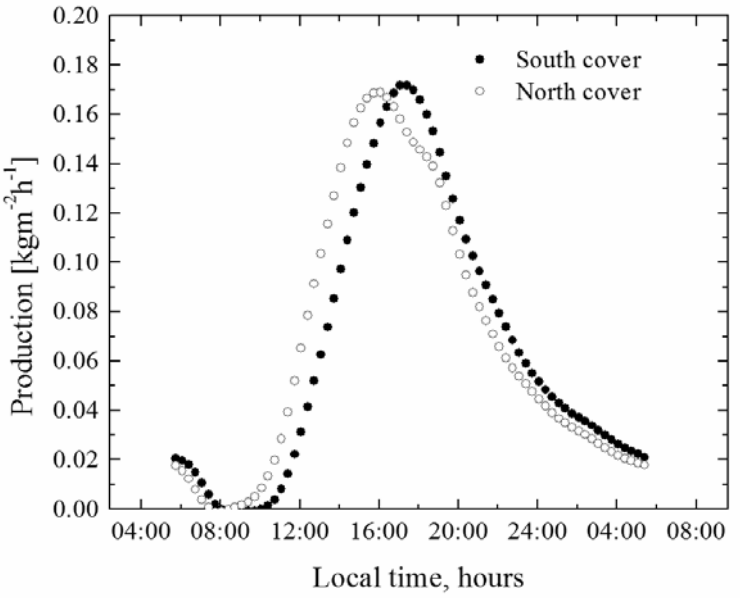

Figure 12. Distillate production with condensers facing a north-south direction in a double-slope condenser solar still (Reprinted from [19], with permission from Elsevier, 2019).

4. Field Experiences in Seawater Solar Distillation

Freshwater scarcity is a big issue in coastal and isolated communities of Baja California Sur in Mexico. This fact and the abundance of seawater in this region is the main motivation to undertake research on low-maintenance water desalination plants. Single-effect solar stills are a practical solution to this problem.

Research efforts have led the Mexican working group to the design of solar stills of different sizes and geometries. Figure 13 shows a long channel shallow solar still. It is characterized by a

short distance between the evaporating water and the condenser glass, a wood frame structure with polystyrene thermal insulation, 3.2 mm-thick tempered glass condenser, and a black plastic painting solar collector. Mean distance from the glass condenser to the water surface is 7.2 cm, and the cover has an inclination of 4°. Dimensions are 0.85 m wide and 9.63 m long, with an effective distillation area of 8.18 m^2. Water depth is 20 mm, for which it contains 165 L of brain. The still had a daily production of 40 L of distilled water.



Figure 13. Long channel shallow solar still.

The experimental field solar still apparatus shown in Figure 14 was also built. This is a large cross section double-slope solar still. The still is 3.86 m long, 2.64 m wide and 1.42 m height. A galvanized iron frame supports the glass condensers of 5 mm thick and the basin is a wooden box with low density polystyrene to minimize heat losses. Condensers are tilted 45° and the solar collector is a composite material made from aluminum foil, cotton fabric and black silicon. The implemented solar collector is a rigid, impermeable and sun radiation absorber. The base has a rolling system that provides rotation of 360°, and a production of 3 l/m^2 was obtained. The still was instrumented for measuring wind speed and direction, solar radiation, ambient temperature, distillate yield and temperatures with thermocouple sensors.



Figure 14. Orientation-adjustable large cross-section solar still for outdoor experimentation.

A distinguishing characteristic of a large-dimension solar stills is its large thermal inertia. Figure 15 shows the plot of the distillate yield for this still. As can be noted, the main production is obtained after noon and during night-time hours.

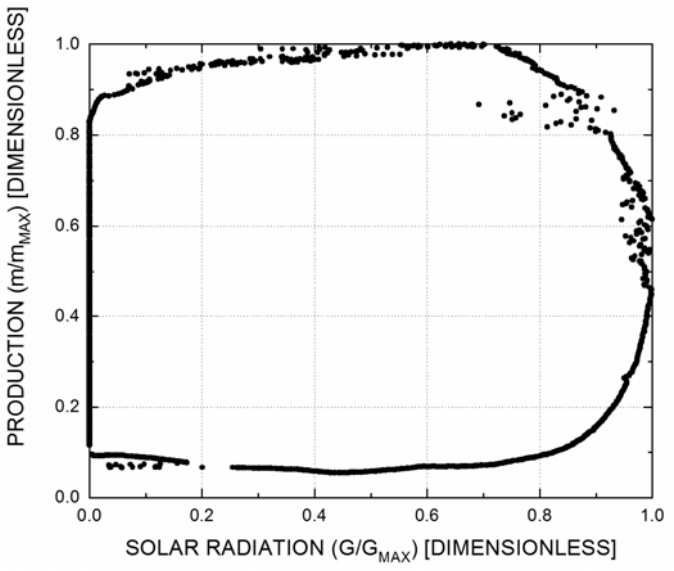

Figure 15. Thermal inertia characteristic of large solar stills.

Another type of solar still is shown in Figure 16. It was assembled with 31 basin modules of ferrocement, made of a steel wire mesh and cement mortar. Dimensions of each module were 1.6 m wide and 1.25 m long, with concrete seamed joints such that each module is a brine container to avoid leakage and dryness of the basin due to the inclination of the long distillation channel. The glass condensers were installed with an inclination of 30°, and the effective distillation area was 54 m^2. Total length of the distillation channel was 38.75 m and on a summer day it produced 200 L of distilled water, or 3.7 l/m^2. Seawater was fed with a mechanical wind water pump from a well on the beach to an elevated water storage tank, that fed the still channels by gravity.



Figure 16. Double slope solar still with ferrocement basin.

Another large cross-section solar still with dimensions 4.4 m wide, 9.4 m long and 2.5 m height is shown in Figure 17. The condenser structure is a wooden frame with 52 glass plates 1.77 m long and 0.77 m wide, 6 mm thick, and inclined 45°. The basin was made of ordinary concrete covered with a solar collector membrane made of silicon, aluminum foil and black cotton fabric. Galvanized iron channels with a slope of 1% were installed at the middle and bottom of each condensing side to collect the distillate. Daily production obtained with this still was 3.5 L/m^2. The still was installed on the highest part of an island called El Pardito, to the south of the island of San José in Baja California Sur.

On this island live a small community of fishermen. The transportation of the materials and a portable concrete cement mixer on a panga—a small fishing boat—was one of the major difficulties faced.



Figure 17. Large cross-section solar still with wood-supported glass condensers and concrete base materials.

Finally, a ferrocement basin long channel solar still is shown in Figure 18. The desalination system was installed in a coastal fishermen community of 100 inhabitants in Puerto Chale, Baja California Sur. It consisted of six long distillation channels, each 1.6 m wide and 40 m long. Seawater was pumped from a beach well with an aerogenerator and a solar electric water pump. Daily production of 1000 L was expected, enough to address the more urgent freshwater needs of the people.



Figure 18. Solar desalination plant in Puerto Chale, Baja California Sur, Mexico.

5. Mass Production Manufacturing of Solar Stills with Technology Innovations

Single-effect solar stills found in the market are relatively unattractive due to the lack of a mass production manufacturing processes of efficient distillation apparatus. Most of the solar stills reported in the literature are hand-crafted. Efficient distillation prototypes require various components, like walls with thermal insulation, a solar collector plate or membrane, a rigid structure, a glass or plastic condenser, and no less important, environmentally friendly materials. This fact makes it difficult to find

an adequate and practical manufacturing process. However, various manufacturing methodologies and materials can be found in the literature. A recent paper reviews the use of plastics and recycled materials [20]. Some stills are made of polyethylene terephthalate (PET) bottles for the basin and the condensing surface [21]. The thermoforming process has also been applied in the design of solar stills, where heat and a mold are used to give shape to a black high-density sheet of polyethylene. Walls are thin, so it is not possible to embed thermal insulation [22].

The use of the industrial rotational molding process in the manufacturing of solar stills may overcome these limitations. This process permits the mass production of solar stills, and the inclusion of technology innovations in the manufactured parts. Some innovations are the possibility of embedding thermal insulation in the structure of the still, a single-piece or monolithic still, integrated distillate collector channel and distillate yield container, black polyethylene that avoids the use of an additional solar collector plate, environmentally friendly materials, and the possibility of using a glass or film polyethylene condenser.

The rotational molding process is shown in Figure 19. This is a 4-step process in which a hollow mold is filled with polyethylene powder, closed and moved to an oven; the mold is heated in the oven for melting the polymer, adhering it to the wall, and rotated biaxially for an even dispersal and consistent product wall thickness; then, the mold is cooled with water or air; and finally, the part is removed from the mold for inspection, assembly or packaging operations.

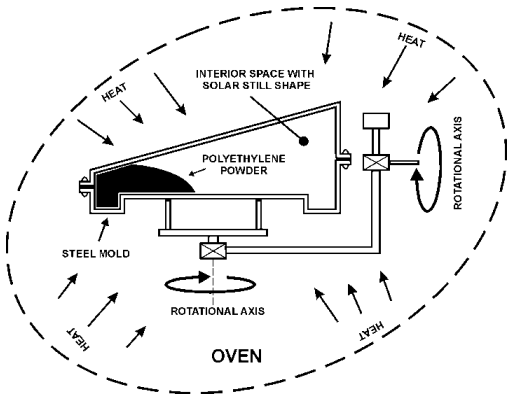

Figure 19. Rotational molding process for manufacturing of innovative solar stills.

Under this process, a solar still composed of two pieces can be produced, as shown in Figure 20. The main structure is a one-piece part, made of black rigid polyethylene, so it is water-leak resistant and serves as the solar collector. Therefore, it does not need a separate solar collector plate or material.

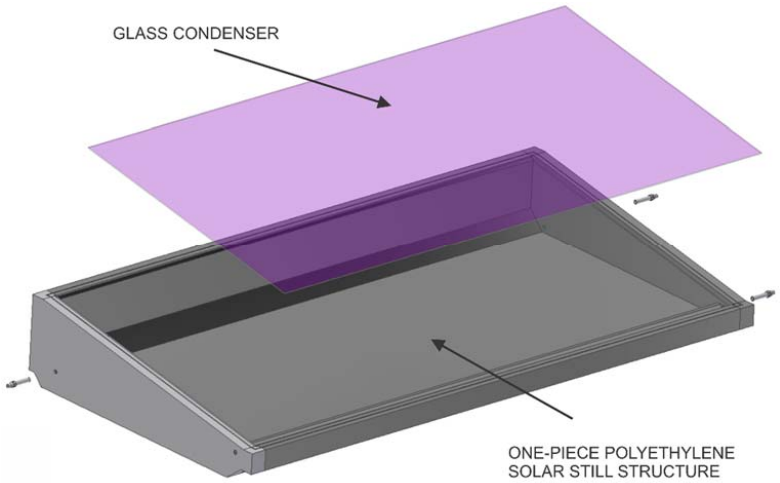

Figure 20. Two-piece innovative polyethylene solar still.

This process produces a hollow part, for which it is straightforward to undertake an injection process to fill the interior of the structure with polyurethane foam as thermal insulation, as shown in Figure 21, in order to avoid major energy loses.



Figure 21. Hollow still to embed thermal insulation.

Concerning other innovations of this product, under this process the mold can be fabricated so that the distillate yield container is also integral part of the still as shown in Figure 22. The distillate runs over the inner surface of the glass condenser and is deposited directly in the water container tank. The rotomolding manufacturing process is very flexible. Instead of an integral distillate collector tank, a solar still can be designed with the commonly used water collector channel, located at the lower part of the condensing plate, to collect the distilled water and transport it to an external water bottle through a freshwater drain port.

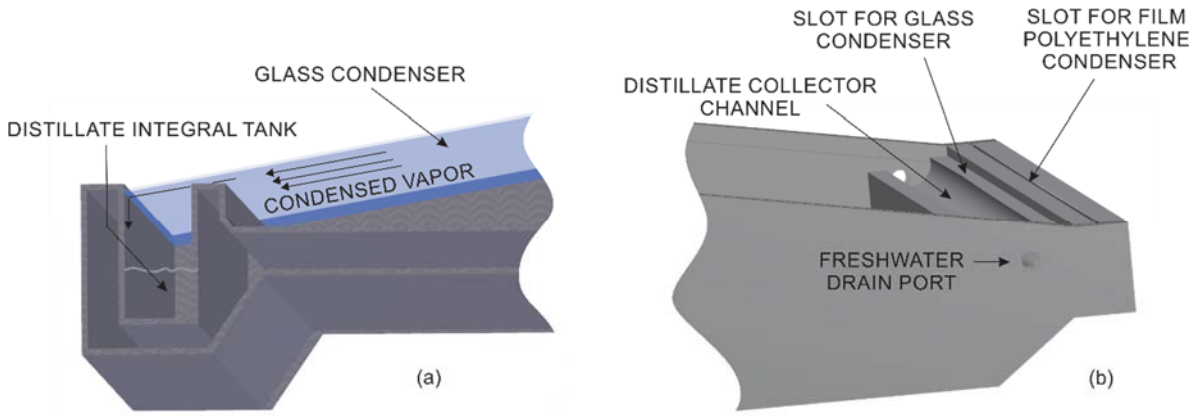

Figure 22. Integrated distillate water container (**a**), and the commonly used distillate yield collector channel to drain the condensed water to an external container (**b**).

The authors of the present paper did not find reports in the literature on the use of the rotational molding process in the manufacture of solar stills.

6. Conclusions

This paper illustrates the vast knowledge that has been accumulated over the years in designing, building and operating single-effect passive solar stills in Mexico. Experience has also been built in operating and maintaining these stills, to mitigate much needed freshwater requirements in the northern semi-desert parts of Mexico. The next step will very likely consist in evolving construction by means of an industrial process that can take advantage of polymeric materials, possibly manufactured with recycled plastics. As shown in the previous section, such a design can incorporate innovations, such as a very regular and standard geometry, artificial intelligence for loading, operating and maintaining the still, and probably constructing industrial-sized distilling operations, by simply putting together

a large number of solar stills. The experience of the authors indicates that such an effort is in order with current technical capacity and water costs. The present government administration has let it be known that such a project could aim at official and international funding. Mexico can thus become an international leader in solar distillation of seawater.

Author Contributions: Conceptualization, E.R., J.L.F.-Z. and M.A.P.-G.; methodology, E.R., J.L.F.-Z. and M.A.P.-G.; software, E.R.; validation, E.R. and M.A.P.-G.; formal analysis, J.L.F.-Z. and M.A.P.-G.; investigation, E.R., J.L.F.-Z. and M.A.P.-G.; resources, E.R. and M.A.P.-G.; data curation, E.R.; writing—original draft preparation, E.R.; writing—review and editing, J.L.F.-Z. and M.A.P.-G.; visualization, E.R. and M.A.P.-G.; supervision, J.L.F.-Z.; project administration, E.R., J.L.F.-Z. and M.A.P.-G. All authors have read and agreed to the published version of the manuscript.

Funding: This research received no external funding.

Conflicts of Interest: The authors declare no conflict of interest.

Nomenclature

Symbols

C	Thermal capacity, J m^{-2} K^{-1}
G	Total solar radiation, W m^{-2}
h	Heat transfer coefficient, W m^{-2} K^{-1}
h_{fg}	Latent heat of vaporization, J kg^{-1}
H	Corresponding fraction of absorbed radiation, W m^{-2}
k_{ext}	Extinction coefficient, m^{-1}
L	Wall thickness, m
m''	Mass flow rate, kg m^{-2} s^{-1}
n	Day of year
N	Number of daylight hours
Nu	Nusselt number, dimensionless
P	Partial pressure of water vapor, N m^{-2}
Pr	Prandtl number, dimensionless
q	Heat flow rate, W m^{-2}
r	Reflected portion, dimensionless
Ra	Rayleigh number, dimensionless
R_b	Ratio of beam radiation for tilted surfaces
t	Time, s
T	Temperature, K
U	Global heat transfer coefficient, W m^{-2} K^{-1}
v	Wind speed, m s^{-1}

Greeks

α	Absorptance, dimensionless
β	Cover slope, °
γ	Azimuth, °
δ	Sun declination, °
ε	Emittance, dimensionless
ϕ	Latitude, °
θ	Angle of incidence, °
ρ	Reflectance, dimensionless
σ	Stefan–Boltzmann constant, 5.6697×10^{-8} W m^{-2} K^{-4}
τ	Transmittance, dimensionless
ω	Hour angle, °

Subscripts

a	Absorption
b	Bottom, beam radiation
c	Convective
e	Environment
g	Glass
r	Radiative
s	Sky
w	Water
z	Zenithal
$\parallel$	Parallel component of unpolarized radiation
$\perp$	Perpendicular component of unpolarized radiation

References

1. Telkes, M. Fresh water from sea water by solar distillation. *Ind. Eng. Chem.* **1953**, *45*, 1108–1114. [CrossRef]
2. Kaviti, A.K.; Kumar, A.; Prakash, O. Effect of design parameters on productivity of various passive solar stills. In *Solar Desalination Technology*; Kumar, A., Prakash, O., Eds.; Springer: Singapore, 2019; pp. 49–73.
3. Al-harahsheh, M.; Abu-Arabi, M.; Mousa, H.; Alzghoul, Z. Solar desalination using solar still enhanced by external solar collector and PCM. *Appl. Therm. Eng.* **2018**, *128*, 1030–1040. [CrossRef]
4. Cooper, P.I. The absorption of radiation in solar stills. *Sol. Energy* **1969**, *12*, 33–346. [CrossRef]
5. Fernandez, J.L.; Chargoy, N. Multi-stage, indirectly heated solar still. *Sol. Energy* **1990**, *44*, 215–223. [CrossRef]
6. Duffie, J.; Beckman, W. *Solar Engineering of Thermal Processes*; John Wiley and Sons Inc.: New York, NY, USA, 1991.
7. Watmuff, J.H.; Charters, W.W.S.; Proctor, D. Solar and wind induced external coefficients solar collectors. *Rev. Int. Heliotech.* **1977**, *2*, 56.
8. Sharma, V.B.; Mullick, S.C. Estimation of heat-transfer coefficients, the upward heat flow, and evaporation in a solar still. *ASME J. Sol. Energy Eng.* **1991**, *113*, 36–41. [CrossRef]
9. Bejan, A.C. *Convection Heat Transfer*; John Wiley and Sons Inc.: New York, NY, USA, 1995.
10. Dunkle, R.V. Solar water distillation: The roof type still and a multiple effect diffusion still. In *International Developments in Heat Transfer, Int. Heat Transfer Conference, Part 5*; University of Colorado: Boulder, CO, USA, 1961; pp. 895–902.
11. Porta-Gándara, M.A.; Fernández-Zayas, J.L.; Chargoy-del-Valle, N. Solar still distillation enhancement through water surface perturbation. *Sol. Energy* **2020**, *196*, 312–318. [CrossRef]
12. Rubio, C.E.; Fernández, J.L. Experimental study of an orientable large cross-section solar still. In *XXVII Semana Nacional de Energía Solar*; Ecosur: Chihuahua, Mexico, 2003; pp. 337–341.
13. Rubio, E.; Porta, M.A.; Fernández, J.L. *Cavity Geometry Influence on Mass Flow Rate for Single and Double Slope Solar Stills. Applied Thermal Engineering*; Elsevier: Amsterdam, The Netherlands, 2000; Volume 20, pp. 1105–1111.
14. Rubio, E.; Fernández, J.L.; Porta-Gándara, M.A. Modeling thermal asymmetries in double slope solar stills. *Renew. Energy* **2004**, *29*, 895–906. [CrossRef]
15. Belhadj, M.M.; Bouguettaia, H.; Marif, Y.; Zerrouki, M. Numerical study of a double-slope solar still coupled with capillary film condenser in south Algeria. *Energy Convers. Manag.* **2015**, *94*, 245–252. [CrossRef]
16. Poulikakos, D.; Bejan, A. The fluid dynamics of an attic space. *J. Fluid Mech.* **1983**, *131*, 251–269. [CrossRef]
17. Baum, V.A.; Bairamov, R. Heat and mass transfer processes in solar stills of hotbox type. *Sol. Energy* **1964**, *3*, 78–82. [CrossRef]
18. Rubio, E.; Fernandez, J.L. Parametric analysis of a solar still with inverted V-shaped glass condenser. *Therm. Sci.* **2015**, *19*, S571–S580. [CrossRef]
19. Rubio-Cerda, E.; Porta-Gándara, M.A.; Fernández-Zayas, J.L. Thermal Performance of the Condensing Covers in a Triangular Solar Still. In *Renewable Energy*; Elsevier: Amsterdam, The Netherlands, 2002; Volume 27, pp. 301–308.
20. Arunkuma, T.; Ao, Y.; Luo, Z.; Zhang, L.; Li, J.; Denkenberger, D.; Wang, J. Energy efficient materials for solar water distillation—A review. *Renewable Sustainable Energy Rev.* **2019**, *115*, 109409. [CrossRef]

21. Toyama, S.; Murase, K. Solar stills made from waste materials. *Desalination* **2004**, *169*, 61–67. [CrossRef]
22. Flendrig, L.M.; Shan, B.; Subrahmaniam, N.; Ramakrishnan, V. Low cost thermoformed solar still water purifier for D&E countries. *Phys. Chem. Earth.* **2009**, *34*, 50–54.



© 2020 by the authors. Licensee MDPI, Basel, Switzerland. This article is an open access article distributed under the terms and conditions of the Creative Commons Attribution (CC BY) license (http://creativecommons.org/licenses/by/4.0/).